Multiple scattering in random dispersions of spherical scatterers: Effects of shear-acoustic interactions

Valerie J. Pinfield and Derek Michael Forrester

Citation: J. Acoust. Soc. Am. **141**, 649 (2017); doi: 10.1121/1.4974142

View online: http://dx.doi.org/10.1121/1.4974142

View Table of Contents: http://asa.scitation.org/toc/jas/141/1

Published by the Acoustical Society of America

Multiple scattering in random dispersions of spherical scatterers: Effects of shear-acoustic interactions

Valerie J. Pinfield[a] and Derek Michael Forrester
Chemical Engineering Department, Loughborough University, Loughborough LE11 3TU, United Kingdom

(Received 28 June 2016; revised 6 December 2016; accepted 20 December 2016; published online 31 January 2017)

The propagation of acoustic waves through a suspension of spherical particles in a viscous liquid is investigated, through application of a multiple scattering model. The model is based on the multiple scattering formulation of Luppé, Conoir, and Norris [J. Acoust. Soc. Am. **131**, 1113–1120 (2012)] which incorporated the effects of thermal and shear wave modes on propagation of the acoustic wave mode. Here, the model is simplified for the case of solid particles in a liquid, in which shear waves make a significant contribution to the effective properties. The relevant scattering coefficients and effective wavenumber are derived in analytical form. The results of calculations are presented for a system of silica particles in water, illustrating the dependence of the scattering coefficients, effective wavenumber, speed, attenuation on particle size and frequency. The results demonstrate what has already been shown experimentally; that the shear-mediated processes have a very significant effect on the effective attenuation of acoustic waves, especially as the concentration of particles increases.

[http://dx.doi.org/10.1121/1.4974142]

[ANN] Pages: 649–660

I. INTRODUCTION

The investigation of low frequency (long wavelength) acoustic propagation problems in inhomogeneous media has been pursued for many different systems and applications. Often the objective is to obtain the effective properties of the equivalent homogeneous medium, for ordered or disordered structures. Whilst many acoustic studies focus on ordered structures such as crystals or periodic arrays, the materials of interest in this paper are disordered inhomogeneous media, with random distributions of scatterers in a homogeneous matrix. In elastic systems such as composite materials containing fibers or nanoparticles, homogenization schemes[1] such as effective medium models,[2–4] multiple scattering models[5–8] and the representative volume element approach,[9] as well as computational schemes of various types,[10] have been applied. Related propagation problems occur in porous materials, for which analysis is often based either on Biot-type models,[11–13] effective medium models,[14] multiple scattering approaches,[15] or other homogenization schemes.[16,17] Propagation in systems of resonant scatterers, including bubbles in liquids, have been investigated using multiple scattering models by a number of workers.[18–20] Further interest in the problem of propagation in inhomogeneous media has been prompted by the development of the field of acoustic metamaterials,[21] for which resonant scatterers may be used to achieve modified acoustic properties.[22–25] Some such studies use multiple scattering models to predict wave propagation in the long wavelength system with resonant scatterers.[22,26]

The work reported here concerns propagation through liquid suspensions of solid particles, where the particle locations are only weakly correlated, the particles are non-resonant, and propagation is in the long wavelength region. This type of system has application for particle characterization, for determination of particle size, concentration or density,[27–31] as well as for monitoring processes, such as crystallization,[32–34] and slurries.[35] A number of approaches have been developed for acoustic characterization of dispersions of particles. These include the scattering and absorption models of Dukhin;[36,37] the diffusive acoustic wave spectroscopy method of Aubry and Derode,[38] Leroy and Derode,[39] and Viard and Derode;[40] the combined ballistic/multiple scattering model of Page[41] for resonant scatterers; and backscattering methods (with semi-empirical multiple scattering) such as those developed by Stintz's group.[42,43] Other workers have used the multiple scattering models of Foldy,[44] Waterman and Truell,[45] Fikioris and Waterman,[46] and Lloyd and Berry,[47] to interpret ultrasound measurements in bubbly liquids,[19] particles in liquid suspensions,[22,48,49] and emulsions.[27,50–52] It is these multiple scattering models which form the basis for the present work.

Although liquids are not considered to sustain shear wave propagation, the scattering of compressional waves by particles produces rapidly decaying shear waves in the regions close to the particle surfaces. These contribute significantly to the effective attenuation of the compressional wave mode passing through the suspension of particles.[49,53,54] The effects of the production of shear wave modes and thermal modes at the particle have been incorporated into multiple scattering models[45–47] by use of the Epstein and Carhart[55] or Allegra and Hawley[56] (ECAH) formulations for the scattering coefficient of each individual

[a]Electronic mail: v.pinfield@lboro.ac.uk

particle.[48] But the influence of shear and thermal waves on *neighboring* particles has commonly been neglected in the multiple scattering models, which consider only the acoustic (compressional) mode in the multiple scattering analysis.[45–47] Although the effect of shear waves on compressional wave propagation has been addressed for solid materials (cylindrical scatterers),[8] these effects have routinely been neglected in liquid systems, although experimental evidence for their importance has been known for some time.[49]

Hipp *et al*. proposed a core-shell model to account for thermal and shear effects on neighboring particles, through an effective scattering coefficient.[57] Their model compared favorably with experimental data.[49] Thermal effects were also considered many years ago by Isakovich,[58] and later incorporated into a multiple scattering formulation through a core-shell model by Hemar *et al*.[59] and McClements *et al*.[60] Other workers (including one of the current authors) have applied an effective medium approach to the problem of shear wave interactions, through the use of an effective density and viscosity for the material surrounding the scatterers.[53,54] However, it proved difficult to identify effective properties which provided the correct limiting behavior where shear and thermal effects are negligible. Alba used a stochastic numerical solution to the multiple scattering problem with three wave modes (compressional, thermal, and shear)[61] and the associated software is commercially available.

In 2012, Luppé *et al*. published a new multiple scattering model[62] based on the Waterman and Truell model,[45] but including the effects of thermal and shear wave modes on multiple scattering. One of the current authors has since applied the model to emulsions (liquid droplets in a liquid), in which thermal effects are the dominant mode-conversion mechanism contributing to multiple scattering.[63,64] More recently, the current authors have studied the shear wave multiple scattering by applying the model of Luppé *et al*. to suspensions of solid particles in a liquid. In this system, shear waves are believed to have a significant effect on compressional mode propagation. Papers presenting the comparison of the model with *experimental* results have already been published,[65,66] but here the model of the propagation is examined in more depth, demonstrating the dependence of scattering coefficients on the shear wavenumber, and the resulting influence on the effective wavenumber. In Sec. II, the model for scattering in a liquid suspension of solid particles is presented, developed from the formulation of Luppé *et al*. for an effective wavenumber.[62] Analytical solutions for the relevant scattering coefficients (transition factors) are presented in Sec. II C and II D. The mathematical model is then explored through numerical calculations in Sec. III, illustrating the dependence of the scattering coefficients and effective properties on particle size and frequency. Finally, velocity and attenuation spectra are presented to demonstrate the impact of shear effects on spectroscopy measurements, in comparison with the Lloyd-Berry model without these shear effects. Comparison with experimental data is presented elsewhere.[65,66]

II. THE MODELS

A. Multiple scattering

The development follows closely the approach adopted for thermo-elastic scattering detailed in a previous paper,[63] which was based on the multiple scattering formulation of Luppé *et al*.[62] Only the main results are outlined here and the reader is referred to the previous papers for a fuller explanation. Taking the "low concentration expansion" presented by Luppé *et al*.[62] [Sec. V A, Eqs. (29)–(32)], the effective wavenumber, K_1, for compressional wave propagation is written as

$$K_1^2 = k_1^2 + \varepsilon y_1^{(1)} + \varepsilon^2 y_1^{(2)}, \tag{1}$$

where k denotes the wavenumber of the continuous phase and the numerical subscript denotes the wave mode, taking the values 1, 2, 3 for compressional, shear, and thermal wave modes, respectively. The concentration is represented by $\varepsilon = -4in_0 = -3i\phi/(\pi a^3)$ which relates to the number density of particles in the suspension, n_0, where ϕ is volume fraction and a is the particle radius. The contributions to the effective wavenumber are expressed in terms of the transition factors, which define the scattering process and mode conversions, at a single particle. The transition *operator* $T^{pq}(\mathbf{r}_j)$ defines the scattered field at a single particle due to an exciting field, thus

$$\varphi_S^{(q)}(\mathbf{r}, \mathbf{r}_j) = T^{pq}(\mathbf{r}_j)\varphi_E^{(p)}(\mathbf{r}, \mathbf{r}_j), \tag{2}$$

where $\varphi_S^{(q)}(\mathbf{r}, \mathbf{r}_j)$ is the potential of the scattered wave field of mode q at location $\mathbf{r}$ produced by a scatterer at $\mathbf{r}_j$ due to an exciting field of mode p with the potential $\varphi_E^{(p)}(\mathbf{r}, \mathbf{r}_j)$. If the exciting and scattered fields are defined in terms of Rayleigh partial wave expansions (solutions of the Helmholtz equation in spherical polar coordinates), the transition operator can then be replaced with a transition *factor* T_n^{pq} for each partial wave order, thus giving

$$T^{qp}(\mathbf{r}_j) j_n(k_q\rho_j) P_n(\cos\theta) = T_n^{qp} h_n(k_p\rho_j) P_n(\cos\theta), \tag{3}$$

where $j_n(kr_j)$ and $h_n^{(1)}(kr_j)$ are the spherical Bessel and Hankel functions (of the first kind throughout), respectively, $\boldsymbol{\rho}_j = \mathbf{r} - \mathbf{r}_j$, and $P_n(\cos\theta)$ are the Legendre polynomials.The contributions to the effective wavenumber at the first order in concentration include only compressional-compressional transition factors; these are all included in the Lloyd-Berry multiple scattering formulation[47] and are defined by the terms

$$y_1^{(1)} = M_{11}^{(0)}, \tag{4}$$

where

$$M_{qp}^{(0)} = \frac{\pi}{\sqrt{k_p k_q}} \sum_{n=0}^{\infty} (2n+1) T_n^{qp}. \tag{5}$$

No mode conversion terms appear at first order in concentration. However, at second order in concentration, mode

conversion terms are significant, and appear through $y_1^{(2)}$ [for compressional mode propagation, Eq. (1)],[62]

$$y_1^{(2)} = M_{11}^{(1)} + \sum_{q\neq 1} \frac{M_{1q}^{(0)} M_{q1}^{(0)}}{\left(k_1^2 - k_q^2\right)}, \tag{6}$$

$$M_{pp}^{(1)} = \frac{\pi}{k_p} \sum_{q=1}^{3} \sum_{n=0}^{\infty} \sum_{\nu=0}^{\infty} (-1)^{n+\nu} (2n+1) \times (2\nu+1) T_n^{qp} \bar{Q}_{n\nu}^{(q)}(k_p) T_\nu^{pq}. \tag{7}$$

In order to identify the mode-conversion contributions, only the terms with transition factors T_n^{pq} with $p \neq q$ are presented here. It has previously been shown that the low concentration expansion of Luppé *et al.*[62] leads to the Lloyd-Berry expression for effective compressional wavenumber when only compressional-compressional scattering coefficients are retained, and particles are assumed to be randomly distributed outside the excluded volume of the hard sphere particles. These terms are not considered further in this work. For $p \neq q$,

$$\bar{Q}_{n\nu}^{(q)}(k_p) = \frac{i\pi b}{\left(k_p^2 - k_q^2\right)} (-1)^{n+\nu} \left\{ \frac{i}{k_q b} + \sum_{l=0}^{\infty} G(0,\nu;0,n;l) \times \left[k_p b j_l'(k_p b) h_l(k_q b) - k_q b j_l(k_p b) h_l'(k_q b) \right] \right\}, \tag{8}$$

where b is radius of the excluded volume around a single particle.[62] The subscripts and indices n and ν denote partial wave orders, and $G(0,\nu;0,n;l)$ are the Gaunt coefficients defined by

$$P_n^m(\cos\theta) P_\nu^\mu(\cos\theta) = \sum_{l=0}^{\infty} G(m,n;\mu,\nu;l) P_l^{m+\mu}(\cos\theta).$$

There is no summation over repeated indices in these expressions.

The equations in this section (from Luppé *et al.*[62]) are the basis for the determination of the additional contributions of shear-acoustic multiple scattering to the effective compressional wavenumber in a suspension of solid particles.

B. Shear-acoustic multiple scattering

Now, the contributions of compressional to shear mode conversions (and vice versa) are identified in the effective compressional wavenumber. At second order in concentration, the relevant contributions are those representing the production of a shear wave at a particle due to scattering of the incident compressional wave, followed by the interaction of that shear wave at a nearby particle, causing an outgoing compressional wave. At both scattering events, scattered (outward propagating) waves of all three modes are produced. For clarity, wave mode indices p and q are replaced, from here on, by letters C and S (for compressional and shear wave modes, respectively). The wavenumbers for the liquid continuous phase are given by

$$k_C = \omega/c + i\alpha, \quad k_S = (\omega\rho/2\eta)^{1/2}(1+i), \tag{9}$$

where ω is the angular frequency, c is the speed of the compressional wave, α is the attenuation, ρ is the density, and η is the viscosity. It should be noted that the particles may be solid and therefore have a real shear wavenumber $k_S = \omega(\rho/\mu)^{1/2}$, where μ is the shear modulus. T_n^{CS} is the transition factor for an incident compressional wave, producing a scattered shear wave, and T_n^{SC} for an incident shear wave, producing a scattered compressional wave, for partial wave order n.

The following assumptions have been used to derive the additional contributions to the effective wavenumber due to compressional-shear multimode scattering.

(1) The compressional wavelength is much longer than the particle radius; thus only partial wave orders of 0 and 1 need be retained in the effective wavenumber. The shear mode has no zero order partial wave, and therefore only shear contributions from order 1 are considered.
(2) The scattering of the coherent shear wave (the ensemble averaged scattered shear wave fields) by a particle produces a scattered compressional wave field which is dominated by the first partial wave order. Therefore, only the first order transition factor is considered for the incident shear wave field.
(3) Thermal-elastic multiple scattering contributions to the effective wavenumber are omitted here, but could be included as an additional term based on the results which were presented previously.[63]
(4) The coherent wave for the pseudo-shear wave mode has the same symmetry as the shear field produced by the scattering of a planar compressional wave by a single particle. In other words, the vector displacement-potential or velocity-potential has only a non-zero z-component where the z defines the incident compressional wave propagation direction.
(5) No transverse coherent wave is produced by the multiple scattering events. Thus, the transverse wave velocity potential ψ (defined by the expansion $\mathrm{v}_T = \nabla \times \nabla \times \nabla \times \psi$) is assumed to be zero.

No assumption is made regarding the magnitude of the shear wavelength relative to the particle radius. Assumption (2) is related to the scattering of an incident shear wave, a problem which has been studied in solid continuous media,[67] but not, to our knowledge, in liquid continuous media. The first order partial wave is the lowest order at which shear waves contribute. Since transition factors occur in combination (i.e., products $T_n^{CS} T_m^{SC}$) in the compressional effective wavenumber, the dominant contributions must arise from orders with a significant transition factor for the incident compressional wave T_n^{CS}. Assumption (1) states that the compressional wavelength is much larger than the particle radius, and therefore partial wave orders higher than 1 can be neglected for incident compressional waves; hence only T_1^{CS} makes a significant contribution. Therefore, only shear-incidence transition factors, T_m^{SC}, which appear in combination with the *first order* factor T_1^{CS} are included in the analysis.

Assumption (3) is related only to the *multiple* scattering effects of compressional-thermal mode conversions; the standard first-order Lloyd-Berry[47] multiple scattering formulation includes any single-particle thermal effects through the transition factors T_1^{CC} which were determined using the full Epstein and Carhart[55] or Allegra and Hawley[56] single particle scattering analysis with all three modes included. For many suspensions of solid particles in a liquid, thermal effects are negligible. Assumptions (4) and (5) are made in the multiple scattering formulation of Luppe *et al.*[62] based on symmetry arguments, and in order to establish the definition of the transition factor [see Eq. (3)]. Further discussion of the shear coherent field symmetry can be found in Sec. II C below.

The additional contribution of compressional-shear mode conversions to the effective compressional mode wavenumber has been separated from the standard Lloyd-Berry multiple scattering result as follows:

$$\frac{K_C^2}{k_C^2} = \left[\frac{K_C^2}{k_C^2}\right]_{LB} + \Delta^{CS} = \left[\frac{K_C^2}{k_C^2}\right]_{LB} + \phi^2\Delta_2^{CS}\left(\frac{K_C^2}{k_C^2}\right) + \phi^3\Delta_3^{CS}\left(\frac{K_C^2}{k_C^2}\right), \tag{10}$$

where $[K_C^2/k_C^2]_{LB}$ is the Lloyd-Berry expression for an effective compressional wavenumber[47] which includes only compressional wave multiple scattering, given by

$$\left[\frac{K_C^2}{k_C^2}\right]_{LB} = 1 - \frac{3i\phi}{(k_Ca)^3}\left[T_0^{CC} + 3T_1^{CC} + \cdots\right] - \frac{27\phi^2}{(k_Ca)^6}\left[T_0^{CC}T_1^{CC} + 2T_1^{CC}T_1^{CC} + \cdots\right].$$

Here $\phi^2\Delta_2^{CS}(K_C^2/k_C^2)$ and $\phi^3\Delta_3^{CS}(K_C^2/k_C^2)$ represent the additional terms in the second and third order in concentration, respectively, relating to the multiple scattering contributions from compressional-shear mode conversion and back again.

The multiple scattering formulation of Luppé *et al.*,[62] presented in Sec. II A, is now simplified with the assumptions stated above, taking only the transition factors for the first order partial wave in Eqs. (1) and (6)–(8). Using $\Delta_2^{CS}(\chi)$ to represent the *additional* terms in the function or parameter χ which arise from the compressional-shear mode-conversion terms in the second order in concentration, gives

$$\Delta_2^{CS}\left(y_1^{(2)}\right) = \Delta_{CS}\left(M_{CC}^{(1)}\right) + \frac{M_{CS}^{(0)}M_{SC}^{(0)}}{\left(k_C^2 - k_S^2\right)} \tag{11}$$

with

$$M_{CS}^{(0)} = \frac{\pi}{\sqrt{k_Ck_S}}3T_1^{CS}, \quad M_{SC}^{(0)} = \frac{\pi}{\sqrt{k_Ck_S}}3T_1^{SC}, \tag{12}$$

and

$$\Delta_2^{CS}\left(M_{CC}^{(1)}\right) = 9\frac{\pi}{k_C}T_1^{SC}\bar{Q}_{11}^{(S)}(k_C)T_1^{CS} \tag{13}$$

if only the terms in the first partial wave order transition factors are selected, i.e., $n = \nu = 1$. The only non-zero contributions in $\bar{Q}_{11}^{(S)}(k_C)$ are those with $l = 0, 2$,

$$\bar{Q}_{11}^{(S)}(k_C) = \frac{i\pi b}{\left(k_C^2 - k_S^2\right)}\left\{\frac{i}{k_sb} + G_{110}Y_0^{CS} + G_{112}Y_2^{CS}\right\}, \tag{14}$$

where the relevant Gaunt coefficients $G_{n\nu l} \equiv G(0, \nu; 0, n; l)$ take numeric values $G_{110} = 1/3$, $G_{112} = 2/3$, and

$$Y_n^{CS} = k_Cbj_n'(k_Cb)h_n(k_Sb) - k_Sbj_n(k_Cb)h_n'(k_Sb). \tag{15}$$

There are no other contributions in the effective wavenumber at second order in concentration that include the first order transition factor for compressional to shear mode conversion, T_1^{CS}.

Following some simplification, the additional second-order (in concentration) term is given by

$$\Delta_2^{CS}\left(y_1^{(2)}\right) = \frac{3\pi^2bi}{k_C\left(k_C^2 - k_S^2\right)}\left(Y_0^{CS} + 2Y_2^{CS}\right)T_1^{CS}T_1^{SC} \tag{16}$$

and thus the additional terms in the effective wavenumber are given by

$$\Delta_2^{CS}\left(\frac{K_C^2}{k_C^2}\right) = \frac{-9}{\pi^2a^6}\left[\Delta_2^{CS}\left(y_1^{(2)}\right)\right] = -\frac{27i}{(k_Ca)^6}\cdot\frac{k_C^2(k_Cb)}{\left(k_C^2 - k_S^2\right)}\left(Y_0^{CS} + 2Y_2^{CS}\right)T_1^{CS}T_1^{SC}. \tag{17}$$

For the calculations reported here, the radius of the exclusion volume is taken to be twice the particle radius, i.e., $b = 2a$. If the assumption (1) can be extended such that $|k_Cb| \ll 1$ (the compressional wavelength is much larger than the radius of the excluded volume b) then $Y_2^{CS}/Y_0^{CS} = \mathrm{O}(k_Cb)$ and thus Y_2^{CS} can be neglected.

Equation (17) defines the dominant additional compressional-shear multiple scattering contributions to the effective compressional wavenumber in a suspension of solid particles. Analytical expressions for the third order contribution were provided to the authors by Dr. Francine Luppé, and were further simplified by the authors through the application of further assumptions similar to assumption (1), thus retaining only the first order partial wave order transition factors for compressional-shear, shear-compressional, and shear-shear mode conversions. The third order terms represent the initial interaction of the incident compressional wave with a particle, producing a scattered shear wave, which scatters at a nearby particle, producing another scattered shear wave, which then scatters at another particle to produce a compressional wave. This scattered compressional wave then contributes to the coherent compressional wave in the system. The simplified analytical form of the third order term was presented in a previous paper, of which Dr. Luppé was co-author.[65] Both second and third order terms combine with the Lloyd-Berry terms using Eq. (10) to obtain the full shear-acoustic effective wavenumber for propagation of a compressional wave through the suspension of particles.

C. Transition factors

The additional contributions of compressional-shear mode conversion to the attenuation (through the effective wavenumber) are defined in terms of the transition factors (alternatively denoted scattering coefficients) for these mode conversions. These can be obtained following the ECAH formulation[55,56] for scattering by a single particle using either an incident compressional wave (as in the original ECAH method), or an incident shear wave. This formulation results in a boundary condition matrix equation which can be solved for the scattering coefficients. The compressional-shear transition factor T_1^{CS} can be obtained from the ECAH solution for an incident compressional wave (there denoted C_1), although the coefficient of the scattered shear wave was not previously required for the effective wavenumber. For the transition factor involving an incident shear wave, the incident wave was expressed through the vector potential and the general solutions to the Helmholtz equation in spherical polar coordinates as

$$\mathbf{u}_{S,\mathrm{inc}} = \nabla \times \mathbf{A} = \nabla \times (\nabla \times \psi_{S,\mathrm{inc}} r\hat{\mathbf{r}}), \tag{18}$$

where the general solution is

$$\psi_{S,\mathrm{inc}} = \sum_{n=0}^{\infty} \sum_{m=-n}^{n} i^n (2n+1) j_n(k_S r) P_n^m(\cos\theta) \exp(im\phi). \tag{19}$$

For an incident compressional plane wave (the ECAH solution[55,56]), symmetry arguments require that $m = 0$ for the scattered shear field, so that only the azimuthal component $\mathbf{A}_\phi$ of the potential is non-zero. Here, the same symmetry requirement is imposed on the incident shear field, following Luppé *et al.*[62] [listed in Sec. II B as assumption (4)], so we consider potentials of the form

$$\psi_{S,\mathrm{inc}} = \sum_{n=0}^{\infty} i^n (2n+1) j_n(k_S r) P_n(\cos\theta). \tag{20}$$

The boundary condition matrix equation is identical in form to that of the ECAH model,[48,55,56] with only the right hand side (the incident wave components) replaced by the corresponding shear wave terms. The thermal contributions have been neglected, since they are negligible at order $n = 1$ and above.[68] Equation (9) of Challis *et al.*[48] (with a corrected minus sign) can be re-expressed to give

$$[M_{AH4}] \begin{pmatrix} A_n^S \\ C_n^S \\ A'^S_n \\ C'^S_n \end{pmatrix} = \begin{pmatrix} n(n+1) j_n(k_S a) \\ j_n(k_S a) + k_S a j_n'(k_S a) \\ -2n(n+1)[k_S a j_n'(k_S a) - j_n(k_S a)]/(k_S a)^2 \\ [(k_S a)^2 j_n''(k_S a) + (n^2+n-2) j_n(k_S a)] \end{pmatrix}, \tag{21}$$

where the boundary condition matrix M_{AH4} can be found in the appendix of Challis *et al.*,[69] or from Refs. 55 and 56, and only the first four rows and columns are used here due to the neglect of thermal contributions.

In order to explore the dependence of the transition factors on $(k_C a)$ and $(k_S a)$, analytical solutions have been derived in the long compressional wavelength limit $|k_c a| \ll 1$ [assumption (1)]. The reduced boundary matrix equation (4×4) was solved using the symbolic software MAPLE® (MapleSoft) to obtain the transition factor for both incident compressional and shear waves. The resulting transition factors were then expanded as a series in $(k_C a)$ by taking series expansions of the spherical Bessel and Hankel functions in the compressional wavenumbers both inside and outside the particle. The leading order terms are

$$T_1^{CC} = \frac{i\,(k_C a)^3 (\hat{\rho} - 1)\beta_{hS}}{3D}, \tag{22}$$

$$T_1^{CS} = \frac{k_C a(\hat{\rho} - 1)}{D \cdot h_1(k_S a)}, \tag{23}$$

$$T_1^{SC} = -\frac{2i\,(k_C a)^2 k_S a(\hat{\rho} - 1) j_1(k_S a)}{D} \times \left[\frac{h_1'(k_S a)}{h_1(k_S a)} - \frac{j_1'(k_S a)}{j_1(k_S a)}\right], \tag{24}$$

$$T_1^{SS} = -\frac{\lfloor 3\beta_{jS} + 2(\hat{\rho} - 1)\delta_{jS} \rfloor}{D} \frac{j_1(k_S a)}{h_1(k_S a)}, \tag{25}$$

where $\hat{\rho} = \rho'/\rho$ and

$$D = [3\beta_{hS} + 2(\hat{\rho} - 1)\delta_{hS}], \tag{26}$$

$$\beta_{hS} = k_S a \frac{h_1'(k_S a)}{h_1(k_S a)} - 1, \quad \beta_{jS} = k_S a \frac{j_1'(k_S a)}{j_1(k_S a)} - 1, \tag{27}$$

$$\delta_{hS} = k_S a \frac{h_1'(k_S a)}{h_1(k_S a)} + 2, \quad \delta_{jS} = k_S a \frac{j_1'(k_S a)}{j_1(k_S a)} + 2, \tag{28}$$

where a prime denotes the dispersed phase and unprimed quantities the continuous phase, except on Bessel and Hankel functions where the prime represents the derivative.

D. Scaling of transition factors

In order to stabilize the numerical solution of the matrix boundary equation, the coefficients are defined in a scaled form, thus,

$$T_{1\,\mathrm{scaled}}^{CS} = T_1^{CS} \cdot h_1(k_S a), \tag{29}$$

$$T_{1\,\mathrm{scaled}}^{SC} = \frac{T_1^{SC}}{j_1(k_S a)}, \tag{30}$$

$$T_{1\,\mathrm{scaled}}^{SS} = \frac{T_1^{SS} h_1(k_S a)}{j_1(k_S a)}, \tag{31}$$

which removes the dominant functional dependence due to the Hankel and Bessel functions which can be oscillatory, and differ by many orders of magnitude. A similar scaling

was proposed for the stabilization of the ECAH matrix boundary equation by Pinfield previously.[69] These scaled coefficients will also be used to illustrate the functional dependency of the transition factors more conveniently in a graphical manner in Sec. III A.

The equations presented in Sec. II enable the contribution of shear-acoustic multiple scattering to be calculated for propagation of a compressional wave through a suspension of particles. Equations (10) and (17) can be used to determine the effective wavenumber in a suspension, using either the numerical solution of the matrix boundary equations or the analytical solutions presented in Eqs. (22)–(24) in the long wavelength region $|k_c a| \ll 1$. The speed and attenuation for coherent compressional waves through the suspension are related to the effective compressional wavenumber by

$$K_C = \frac{\omega}{c_{\text{eff}}} + i\alpha_{\text{eff}}. \tag{32}$$

III. RESULTS OF CALCULATIONS

Calculations of the shear-acoustic transition factors and contributions to multiple scattering have been carried out using MATLAB®, for a system of silica in water at 25 °C, over a frequency range 0.01–100 MHz. The physical properties used in the calculations are specified in Table I. This system is known to have minimal thermal scattering contributions, and is dominated by dipole scattering, producing shear waves, due to the density difference between the two phases. Compressional wave scattering was accounted for by including transition factors for $n = 0$ (monopole) and $n = 1$ (dipole) and these were obtained using the full ECAH single particle scattering model[48,55,56] which includes conversion into shear and thermal waves. First, the transition factors for scattering at a single particle are examined (Sec. III A), followed by the additional contributions to the effective wavenumber due to the shear-acoustic mode conversions (Sec. III B), and finally their effect on the effective speed and attenuation are presented in Sec. III C.

A. Transition factors (scattering coefficients)

Figure 1 shows the dependence of the transition factors relating to shear-compressional multi-mode scattering on the dimensionless shear wavenumber $\text{Re}(k_S a)$. The transition factors are scaled by the spherical Bessel or Hankel functions (Sec. II D) and also with the dominant dependence on $k_C a$ removed. The product $T_1^{CS} T_1^{SC}$ varies as $(k_C a)^3$ [Eqs. (23) and (24)], a factor which is cancelled in the effective wavenumber [Eq. (17)], noting that $|k_S^2| \gg |k_C^2|$. The remaining terms in the scaled transition factors are functionally dependent on $\text{Re}(k_S a)$ in the long compressional wavelength limit $k_C a \ll 1$.

TABLE I. Physical properties of silica and water at 25 °C used in the simulations (Ref. 48).

	Water	Silica
Sound velocity/m s^{-1}	1497	5968
Density/kg m^{-3}	997	2100
Shear viscosity/Pa s	0.000891	
Shear modulus/GPa		30.9
Thermal conductivity/J m^{-1} s^{-1} K^{-1}	0.595	1.6
Heat Capacity C_p/J kg^{-1} K^{-1}	4179.0	729.0
Expansivity/K^{-1}	0.00021	1.35×10^{-6}
Attenuation factor/Np m^{-1} MHz^{-2}	0.023	2.6×10^{-10}

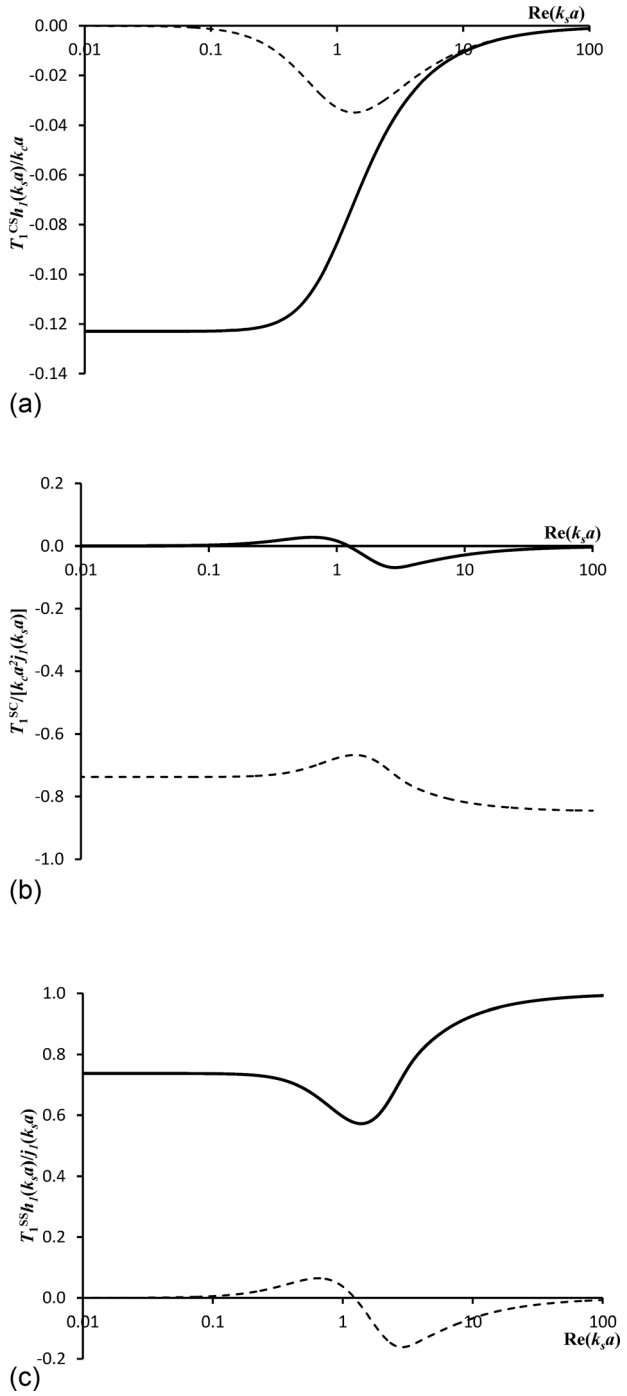

FIG. 1. The real and imaginary parts (solid and dashed lines, respectively) of the scaled transition factors as a function of the real part of the shear wavenumber-radius product $\text{Re}(k_S a)$ calculated using 250 μm diameter silica particles in water at 25 °C: (a) the compressional-shear conversion, $T_1^{CS} h_1(k_S a)/k_C a$, (b) the shear-compressional conversion, $T_1^{SC}/[(k_C a)^2 j_1(k_S a)]$, and (c) the shear-shear conversion, $T_1^{SS} h_1(k_S a)/j_1(k_S a)$.

The results shown in Fig. 1 were calculated for a large particle of 250 μm diameter to ensure that the full range of $(k_S a)$ could be explored within the long compressional wavelength region $(k_C a) \ll 1$. At the upper limit shown, i.e., $\mathrm{Re}(k_S a) = 100$, the compressional dimensionless wavenumber is $\mathrm{Re}(k_C a) = 0.097$. Calculations using smaller particles (of diameters 200 nm and 2 μm) showed that the results were identical within the long wavelength limit, and the curves were indistinguishable where $(k_C a) < 0.1$ and often at higher values of $(k_C a)$. This confirms the dependence of the scaled transition factors with the dimensionless shear wavenumber $(k_S a)$ in the long compressional wavelength region. The analytical results for the transition factors [Eqs. (22)–(24)] were also found to be indistinguishable from those obtained by numerical matrix inversion of the boundary equations within this region. Beyond the long wavelength region, the curves are truncated, and the dependence of the transition factors will be a function of both compressional and shear dimensionless wavenumbers, $(k_C a)$ and $(k_S a)$, respectively. The numerical solution of the boundary equations remains valid in that case but the analytical solutions deviate from the true solution, since they are only valid for small $(k_C a)$.

In all cases, the scaled transition factors approach a constant value at the lower and upper limits of $(k_S a)$ but undergo significant changes with respect to $(k_S a)$ around the "resonance" region $\mathrm{Re}(k_S a) \sim 1$. In the case of an incident compressional wave conversion to a scattered shear wave [Fig. 1(a)] both real and imaginary parts of the transition factor approach zero at the upper limits of $(k_S a)$, and a constant value at low $(k_S a)$, but the imaginary part has a peak around $\mathrm{Re}(k_S a) \sim 1$. This is consistent with the previous observation[56] that a peak in attenuation per wavelength occurs around $\mathrm{Re}(k_S a) \sim 1$, where the scattered shear wave has the greatest impact, and the relative motion of particle and surrounding fluid is greatest. The other transition factors also show the greatest changes at $\mathrm{Re}(k_S a) \sim 1$. Since it is the *combination* of transition factors which contributes to the effective wavenumber for the suspension [Eq. (17)], the effects are likely to be most significant around $\mathrm{Re}(k_S a) \sim 1$ but the limits at low and high $(k_S a)$ are difficult to establish from the individual transition factors.

B. Effective wavenumber

Having explored the dependence of the transition factors for mode conversion on $k_S a$, the effect of such mode conversions on the effective wavenumber are now investigated. The additional contributions to the effective wavenumber (in the form K_C^2/k_C^2) are presented in Fig. 2. The figure shows both second and third order effects in concentration due to mode conversion between acoustic (compressional) and shear waves. The additional contributions to K_C^2/k_C^2 depend only on the shear wavenumber $k_S a$, because factors of $k_C a$ cancel (see Sec. III A) since $|k_C|^2 \ll |k_S|^2$. The real part of K_C^2/k_C^2 predominantly affects the effective compressional wave speed and the imaginary part the effective attenuation. The calculations were carried out using a particle radius of 1 μm; in this case, the long wavelength criterion $\mathrm{Re}(k_C a) < 0.1$

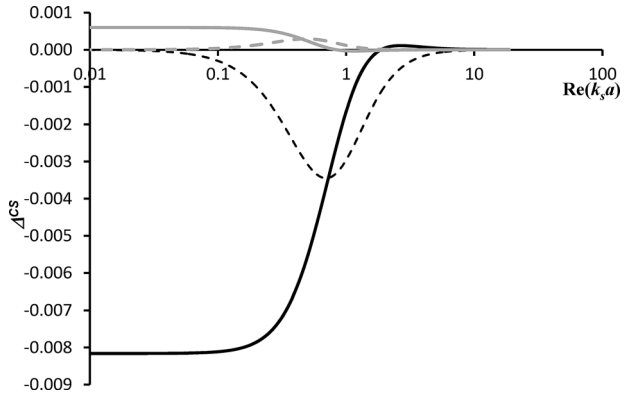

FIG. 2. The real and imaginary parts of the additional contribution to the effective wavenumber due to shear-acoustic multiple scattering, Δ^{CS} [Eqs. (10) and (17)] as a function of $\mathrm{Re}(k_S a)$ for a 10%v/v silica-in-water emulsion with particle radius of 1 μm at 25 °C. The black lines are the second order term $\phi^2 \Delta_2^{CS}$ and the gray lines the third order term $\phi^3 \Delta_3^{CS}$, with the solid and dashed lines showing the real and imaginary parts, respectively, in each case.

corresponds to $\mathrm{Re}(k_S a) < 9.2$, and this covers the range of interest for the additional contributions to the effective wavenumber since they approach zero at large $(k_S a)$. For smaller particles, the long wavelength limit truncates the validity of this curve and some dependence on $(k_C a)$ as well as $(k_S a)$ would be expected outside this region.

All additional mode-conversion effects tend to zero at the large $(k_S a)$ limit, which is equivalent to high frequency for a fixed particle size. Thus, the model predicts that the effective wavenumber approaches the Lloyd-Berry wavenumber at large $(k_S a)$. There are two factors which affect this limit; first, there is little conversion to shear waves in the large $(k_S a)$ limit [see Fig. 1(a)] and second, the shear wave decay length tends to zero in the high frequency limit so shear waves do not reach neighboring particles. Hence multiple scattering with mode conversion between acoustic and shear waves has declining influence on the effective compressional wavenumber at high frequency, large $(k_S a)$.

In the limit of small $(k_S a)$, where the shear wavelength is long compared with the radius of the particle, the imaginary parts of both the second and third order mode conversion contributions tend to zero. These terms therefore have no effect on attenuation in this limit. The real parts, however, tend to a constant value, leading to a persistent effect on effective wave speed in the long shear wavelength limit. Primarily, the trends in the additional mode conversion contributions Δ^{CS} appear to be determined by the dependence of the transition factor T_1^{CS} corresponding to the production of scattered shear waves from the incident compressional wave [see Fig. 1(a)]. The amplitude and phase of the scattered shear wave determines the strength of its interaction with neighboring particles. The greatest energy conversion into the shear mode occurs in the region $\mathrm{Re}(k_S a) \sim 1$. The multiple scattering events are also affected by the shear wave decay length which is long at small $(k_S a)$, so that shear waves can reach neighboring particles even at relatively low concentrations, and become vanishingly small at the large $(k_S a)$ limit, so that the waves do not reach neighboring particles. The combination of the amplitude of the scattered

shear wave, and the distance over which it decays both contribute to the dependence of the effect of shear-acoustic multiple scattering on shear wavelength [through $(k_S a)$].

The only third order terms (in concentration) included here correspond to three-stage scattering events relating to the sequence of mode conversions as follows: compressional-shear, shear-shear, and shear-compressional corresponding to the product of transition factors T_1^{CS}, T_1^{SS}, and T_1^{SC}. Other three-stage events were found to have negligible effect on the effective wavenumber in comparison.

C. Effective speed and attenuation

The effective wave speed and attenuation can be expressed approximately as

$$\frac{\Delta^{CS}(c_{\text{eff}})}{c_{\text{eff}}} \approx -\text{Re}\left(\Delta^{CS}\left(K_C^2/k_C^2\right)\right), \tag{33}$$

$$\Delta^{CS}(\alpha_{\text{eff}}) = \frac{\omega c_{\text{eff}}}{2c^2}\,\text{Im}\left(\Delta^{CS}\left(K_C^2/k_C^2\right)\right). \tag{34}$$

Therefore, both the effective speed, c_{eff}, and the effective attenuation divided by frequency, α_{eff}/f (proportional to attenuation per wavelength of the compressional wave in the continuous phase medium) are functions of the dimensionless shear wavenumber $k_S a$. These are plotted in Fig. 3 for a suspension of particles of radius 1 μm.

In the short shear wavelength limit (large $k_S a$), both speed and attenuation approach the limit given by the acoustic-only multiple scattering model (Lloyd and Berry) for the reasons noted in Sec. II. In this case, the second order (in concentration) multiple scattering contributions in the Lloyd-Berry formulation are small (though significant in speed), but the additional effects due to compressional-shear mode conversions are relatively large, even at this concentration (10v/v%). The contributions to effective speed are dominant in the long shear wavelength region, causing a fixed increase in the speed in the low $k_S a$ limit. This corresponds to the real part of the effective wavenumber contribution shown in Fig. 2. In this system, the mode-conversion terms have little effect on the speed above $\text{Re}(k_S a) \sim 1$.

The effect of mode conversion is to reduce the attenuation [Fig. 3(b)] across the range of $k_S a$ but with rapidly reducing effect at large $k_S a$. The second order terms due to mode conversion reduce the attenuation because the energy in the scattered shear waves, which was assumed to be dissipated near the scatterer in the Lloyd-Berry model, is reconverted in part into the compressional wave mode, thus reducing the effective losses. The third order terms increase the attenuation, accounting for the incomplete nature of the retrieval of the shear wave energy when only second order (two-stage) scattering events are considered. The curve of attenuation divided by frequency [Fig. 3(b)] also displays a shift in the value of $\text{Re}(k_S a)$ at which the peak occurs. Inclusion of multimode multiple scattering reduces the level of the peak and shifts it to a higher value of $\text{Re}(k_S a)$.

Having studied the dependence of the effective speed and attenuation over several decades of the dimensionless shear wavenumber, these properties are now shown over a more limited frequency range typical of experimental measurements (Fig. 4). The results are shown for a silica in water suspension with 400 nm diameter particles at 25 °C for frequencies up to 20 MHz and for concentrations up to 20% by volume. In the frequency range 1–20 MHz, the value of $\text{Re}(k_S a)$ ranges from 0.38 to 1.68, covering the region in which shear effects are expected to be strong. It is clear that above 5% concentration, the effect of the shear mode multiple scattering on the attenuation spectra is very significant, causing a reduction of 20% in the attenuation at 20 MHz when the concentration is 20v/v%. The reduction in attenuation is persistent across the entire spectrum in the range shown. However, the effect on speed is most significant at the lower frequency end of the spectrum, and indeed the spectra with shear multiple scattering converge to those for the Lloyd-Berry model at the upper frequency limit shown. At the highest concentration shown (20% by volume), the reduction in speed is around 20 m s^{-1} for a 20v/v% suspension at 2 MHz.

These results show that the contributions of shear wave modes *must* be accounted for by any multiple scattering model used to interpret experimental measurements where $\text{Re}(k_S a)$ is not large. The Lloyd-Berry model works well (accounting only for acoustic multiple scattering) only where

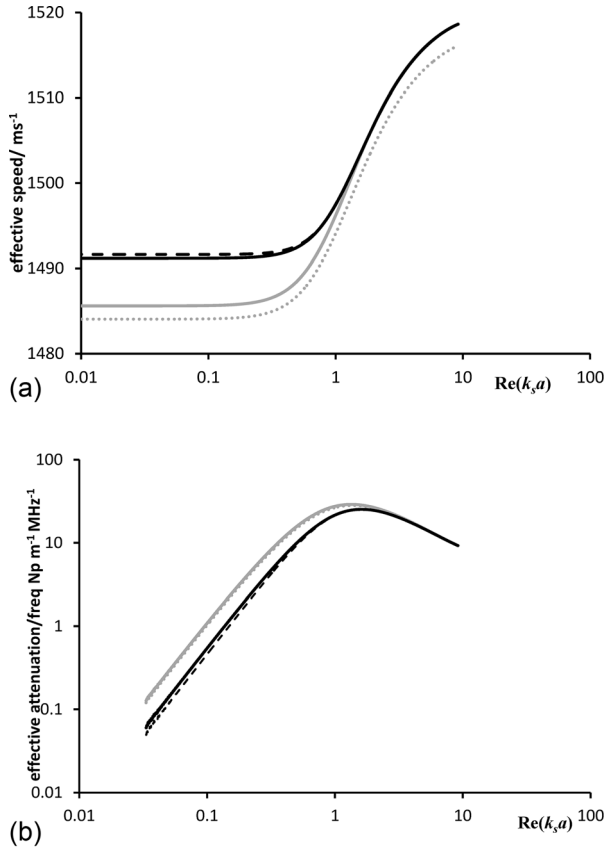

FIG. 3. Effective speed (a) and attenuation divided by frequency (b) as a function of the real part of the shear wavenumber-radius product $\text{Re}(k_S a)$ for a 10v/v% silica-in-water emulsion with a particle radius of 1 μm at 25 °C. The lines shown are for Lloyd and Berry to first order in concentration (gray dotted line), Lloyd and Berry to second order in concentration (gray line), with shear-acoustic multiple scattering to second order in concentration (black dashed line), and to third order in concentration (black solid line).

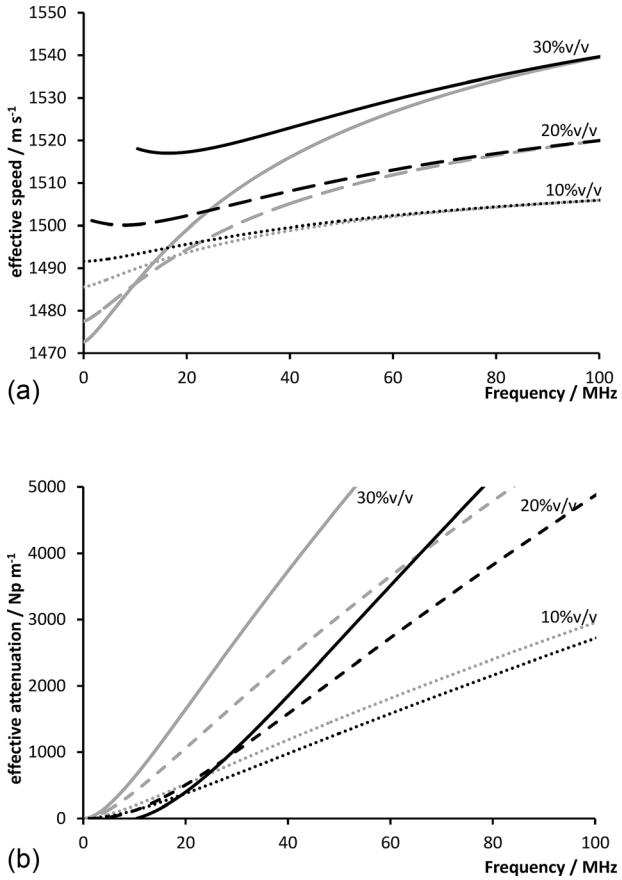

FIG. 4. Effective speed (a) and attenuation (b) as a function of frequency for a silica-in-water emulsion with a particle radius of 100 nm at 25 °C comparing the Lloyd-Berry model (gray lines) with the shear multiple scattering model to second order in concentration (black lines). The speed and attenuation are shown for concentrations of 10% (dotted), 20% (dashed), and 30% (solid) by volume.

$\mathrm{Re}(k_S a)$ is very large, i.e., short shear wavelength and very small shear decay length or at low concentrations. Here, the shear multiple scattering model does not deviate strongly from the Lloyd-Berry model when the concentration is only 5v/v% and therefore the Lloyd-Berry model could be used at low concentrations. However, this concentration limit becomes more restrictive at lower frequencies and/or smaller particle sizes, since, in these conditions, the shear decay length is increased or the distance between particles is reduced (at the same volume fraction), respectively.

IV. DISCUSSION

A recent experimental study of silica in water suspensions[65] demonstrated that the multi-mode multiple scattering model agrees well with experimental measurements for a frequency range 1–20 MHz and particle diameters in the range 100–1000 nm up to concentrations of 20v/v%. The additional contributions in the model appear to account well for the effects of multiple scattering events involving mode conversions between acoustic and shear wave modes. The model provides an analytical solution for the effective wavenumber (although the boundary equations for the transition factors are often solved numerically). Previous attempts to solve the multiple mode scattering problem involved either a stochastic numerical method[61] or a complex 12×12 matrix boundary equation within a hybrid multiple scattering/effective medium model.[57] Hence the model can be considered successful within a defined range of frequency, particle size and concentration.

However, under some conditions, the shear multi-mode scattering model predicts speed and attenuation which is not considered physically realistic. The problems occur particularly where the shear mode effects are strong, namely, at low frequency, small particle size, and high concentrations. As an example, Fig. 5 shows the predicted attenuation as a function of concentration (in the form of volume fraction) at selected frequencies from 1 to 10 MHz [$0.38 < \mathrm{Re}(k_S a) < 1.19$] for the same silica in water suspension studied previously (Fig. 4) with particle diameter 400 nm. Although the Lloyd-Berry elastic multiple scattering model predicts a near-linear trend of attenuation with concentration, the shear scattering model predicts a non-linear dependence, with a much-reduced attenuation. The attenuation curves reach a peak at a certain concentration, above which the attenuation decreases with increasing concentration. This feature is, in itself, physically realistic. As the concentration increases, the loss of energy from the compressional (acoustic) wave mode becomes stronger as more particles are present per unit volume; scattering at each particle leads to a conversion into shear modes, resulting in viscous dissipation. Thus, an increase in concentration results in higher attenuation in both the acoustic-only multiple scattering model, and in the shear scattering model, at low concentrations. The shear wave multiple scattering enables some of the energy assumed to be lost in viscous dissipation, to be reconverted into a compressional wave, resulting in reduced attenuation. However, above a certain concentration, the effects of increased scattering due to the addition of more particles is more than balanced by the reduction in the separation between the particles, which permits shear waves to be scattered at neighboring particles. Thus, the attenuation starts to decrease as the concentration increases. Such dependence

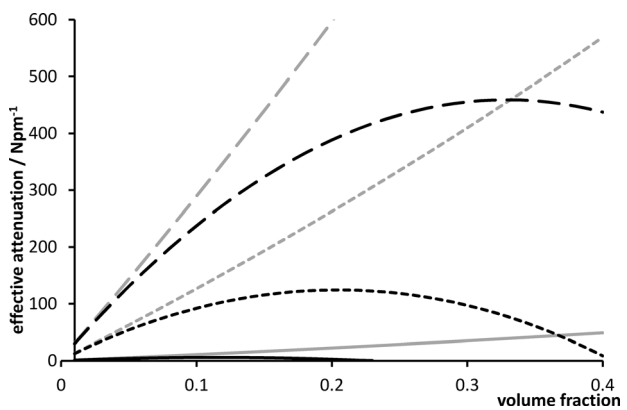

FIG. 5. Effective attenuation as a function of concentration (volume fraction) for a silica-in-water emulsion with a particle radius of 200 nm at 25 °C comparing the Lloyd-Berry model (grey lines) with the shear multiple scattering model to second order in concentration (black lines). The attenuation spectra are shown for frequencies of 1 MHz (solid), 5 MHz (dotted), and 10 MHz (dashed).

has been observed experimentally; see, for example, the data of Hipp *et al*. for silica in water suspensions.[49]

However, the shear wave model over-predicts the strength of the effects, resulting in attenuation/concentration curves which turn right over to meet the axis, so that the attenuation is predicted to be zero. This occurs at around 40v/v% at 5 MHz and 22v/v% at 1 MHz for the system shown in Fig. 5. Above the concentration at which the curve meets the axis, the model predictions are interpreted as a negative velocity, in order to ensure positive attenuation (the imaginary part of K_C^2/k_C^2 is negative), and the attenuation increases sharply again. This behavior, beyond 40v/v%, is not shown in Fig. 5. Although negative phase velocities have been predicted and obtained experimentally for other particulate suspensions in the study of acoustic metamaterials,[22] the effect is not considered to be physically reasonable here. This is because the predicted reduction in attenuation in the shear mode multiple scattering model is a result of reclaiming the energy in the scattered shear wave modes, by reconverting it to the compressional wave in subsequent scattering events at nearby particles. Therefore, it can only be possible to reduce the attenuation by an amount which represents the total energy lost from the compressional wave by viscous dissipation in an acoustic-only multiple scattering model. Hence, the attenuation must not be reduced to zero.

The over-prediction of the shear wave multiple scattering effects are also observed in the effective speed. Figure 4(a) showed the effective speed as a function of frequency, and the curve was truncated for the highest concentration (30 v/v%) to omit the region where the predicted speed is negative. However, the speed can be seen to increase as the frequency decreases just before the truncation point at 10 MHz. A plot of effective speed against concentration is not shown here since it does not illustrate any further effects. Effectively, the shear mode multiple scattering model has a lower frequency limit, a lower particle size limit, and an upper concentration limit to its range of validity. Beyond these ranges the model makes unphysical predictions. The third order (in concentration) terms in the shear mode multiple scattering model do alleviate the problem somewhat, but only act to shift the validity limits slightly. A formula defining the limits of the range of validity has not yet been established.

The causes of the limitations in the model are not yet well understood, but are believed to lie in the non-random nature of the particle locations as the concentration increases. The effective wavenumber formulation obtained by Luppé *et al*.[62] assumed that all particle locations were equally likely outside an excluded volume of radius $2a$ around each particle. The results reported here have been obtained using the Lloyd-Berry model for *acoustic* multiple scattering (in addition to the multimode contributions), and this neglects the excluded volume (taking the limit of infinitely small particles). The effects of excluded volume, and other weak correlations, on *acoustic* multiple scattering have been investigated by other workers, showing only small effects in the long compressional wavelength region.[18,70,71] However, at the high concentrations studied here (especially where the unphysical predictions occur), the effects may be significant and this will subsequently be explored. In addition, the assumption of a simple weak correlation for the multi-mode scattering contributions may be unrealistic for highly concentrated systems. Such an assumption is likely to be increasingly inaccurate as the concentration increases, and a more realistic pair correlation function may be required. The influence of correlations on the effective wavenumber in the long wavelength region may be much stronger in the *shear* multiple scattering case, in which the distance between neighboring particles is critical to the decay of scattered shear waves, and therefore the exciting shear field at the neighboring particle. An increased or decreased probability of particle pairs being within the shear wave decay length is therefore expected to have a significant effect on the effective wavenumber. The investigation of the influence of the pair-correlation function on the effective wavenumber is therefore an area for further study. It may also be the case that some neglected contributions to the effective wavenumber become significant in this region where other terms become much smaller. This needs to be investigated in conjunction with tests of the assumptions made in the analysis (Sec. II B).

V. CONCLUSIONS

This paper has presented a model for propagation of acoustic waves through suspensions of solid particles in a liquid medium, accounting for the effects of shear waves and their contributions to multiple scattering. The model, based on the formulation of Luppé *et al.*,[62] results in an analytical solution for the additional contributions to the effective wavenumber due to the dominant effects of shear wave mode conversion and scattering. Analytical expressions [Eqs. (22)–(25)] have been presented for the transition factors (scattering coefficients) which contribute to the shear-acoustic multiple scattering in the long compressional wavelength region, although numerical solutions can also be obtained.

Calculations using the model show that the shear-acoustic multiple scattering reduces the attenuation, as anticipated, and is consistent with experimental findings. The model correctly approaches the Lloyd-Berry elastic multiple scattering model in the limit of large $(k_S a)$ (short shear wavenumber and decay length). A recent experimental investigation[65] showed very good agreement between the new model and experimental measurements over certain ranges of particle size, concentration, and frequency. However, this paper has also highlighted some difficulties with the model, in which unphysical predictions occur at high concentrations, small particle sizes, and low frequencies. These are believed to be a result of the assumption of a uniform probability distribution function for particle locations, outside the hard-sphere exclusion zone. Further investigation is required to explore the range of validity of the model and the effect of different particle distributions through the pair correlation function. However, the model has provided a formulation and a workable method for the interpretation of ultrasound spectra for smaller particles and higher concentrations than was previously possible using the

elastic-only multiple scattering models. This represents a significant step forward in the application of ultrasonics for process monitoring and for characterization at the nanometer length scales.

VI. DATA

The data for the calculations for silica in water suspensions in this paper are available in Ref. 72.

ACKNOWLEDGMENTS

The work was funded by the EPSRC in the UK, Grant No. EP/L018780/1. The authors are grateful to Dr. Francine Luppé (Le Havre University, France) for helpful discussions and for providing the third order expressions in the effective wavenumber.

[1]N. Willoughby, W. J. Parnell, A. L. Hazel, and I. D. Abrahams, "Homogenization methods to approximate the effective response of random fibre-reinforced composites," Int. J. Solids Struct. **49**, 1421–1433 (2012).
[2]S. K. Kanaun and V. M. Levin, "Propagation of longitudinal elastic waves in composites with a random set of spherical inclusions (effective field approach)," Arch. Appl. Mech. **77**, 627–651 (2007).
[3]J. Kim, "Effective medium theories for wave propagation in two-dimensional random inhomogeneous media," J. Mech. Mater. Struct. **5**, 567–581 (2010).
[4]P. A. Martin, A. Maurel, and W. J. Parnell, "Estimating the dynamic effective mass density of random composites," J. Acoust. Soc. Am. **128**, 571–577 (2010).
[5]J. Kim, "Models for wave propagation in two-dimensional random composites: A comparative study," J. Acoust. Soc. Am. **127**, 2201–2209 (2010).
[6]W. J. Parnell, I. D. Abrahams, and P. R. Brazier-Smith, "Effective properties of a composite half-space: Exploring the relationship between homogenization and multiple-scattering theories," Q. J. Mech. Appl. Math. **63**, 145–175 (2010).
[7]W. J. Parnell and I. D. Abrahams, "Multiple point scattering to determine the effective wavenumber and effective material properties of an inhomogeneous slab," Waves Random Complex Media **20**, 678–701 (2010).
[8]J. Conoir and A. N. Norris, "Effective wavenumbers and reflection coefficients for an elastic medium containing random configurations of cylindrical scatterers," Wave Motion **47**, 183–197 (2010).
[9]M. Ostoja-Starzewski, "Material spatial randomness: From statistical to representative volume element," Prob. Eng. Mech. **21**, 112–132 (2006).
[10]P. Li, Q. Wang, and S. Shi, "Differential scheme for the effective elastic properties of nano-particle composites with interface effect," Comput. Mater. Sci. **50**, 3230–3237 (2011).
[11]F. Meziere, M. Muller, E. Bossy, and A. Derode, "Measurements of ultrasound velocity and attenuation in numerical anisotropic porous media compared to biot's and multiple scattering models," Ultrasonics **54**, 1146–1154 (2014).
[12]M. Fellah, Z. E. A. Fellah, F. G. Mitri, E. Ogam, and C. Depollier, "Transient ultrasound propagation in porous media using biot theory and fractional calculus: Application to human cancellous bone," J. Acoust. Soc. Am. **133**, 1867–1881 (2013).
[13]R. Sidler, "A porosity-based biot model for acoustic waves in snow," J. Glaciol. **61**, 789–798 (2015).
[14]V. T. Potsika, K. N. Grivas, V. C. Protopappas, M. G. Vavva, K. Raum, D. Rohrbach, D. Polyzos, and D. I. Fotiadis, "Application of an effective medium theory for modeling ultrasound wave propagation in healing long bones," Ultrasonics **54**, 1219–1230 (2014).
[15]H. Franklin, F. Luppe, and J. M. Conoir, "Multiple scattering in porous media: Comparison with water saturated double porosity media," J. Acoust. Soc. Am. **135**, 2513–2522 (2014).
[16]K. Gao, J. A. W. van Dommelen, P. Goransson, and M. G. D. Geers, "Computational homogenization of sound propagation in a deformable porous material including microscopic viscous-thermal effects," J. Sound Vib. **365**, 119–133 (2016).
[17]P. Leclaire, O. Umnova, T. Dupont, and R. Panneton, "Acoustical properties of air-saturated porous material with periodically distributed dead-end pores," J. Acoust. Soc. Am. **137**, 1772–1782 (2015).
[18]V. Leroy, A. Strybulevych, J. H. Page, and M. G. Scanlon, "Influence of positional correlations on the propagation of waves in a complex medium with polydisperse resonant scatterers," Phys. Rev. E **83**, 046605 (2011).
[19]V. Leroy, A. Strybulevych, J. H. Page, and M. G. Scanlon, "Sound velocity and attenuation in bubbly gels measured by transmission experiments," J. Acoust. Soc. Am. **123**, 1931–1940 (2008).
[20]O. Lombard, C. Barriere, and V. Leroy, "Nonlinear multiple scattering of acoustic waves by a layer of bubbles," EPL **112**, 24002 (2015).
[21]A. N. Norris and M. R. Haberman, "Introduction to the special issue on acoustic metamaterials," J. Acoust. Soc. Am. **132**, 2783 (2012).
[22]T. Brunet, A. Merlin, B. Mascaro, K. Zimny, J. Leng, O. Poncelet, C. Aristegui, and O. Mondain-Monval, "Soft 3D acoustic metamaterial with negative index," Nat. Mater. **14**, 384–388 (2015).
[23]R. Gracia-Salgado, V. M. Garcia-Chocano, D. Torrent, and J. Sanchez-Dehesa, "Negative mass density and rho-near-zero quasi-two-dimensional metamaterials: Design and applications," Phys. Rev. B **88**, 224305 (2013).
[24]N. Fang, D. Xi, J. Xu, M. Ambati, W. Srituravanich, C. Sun, and X. Zhang, "Ultrasonic metamaterials with negative modulus," Nat. Mater. **5**, 452–456 (2006).
[25]D. M. Forrester and V. J. Pinfield, "Shear-mediated contributions to the effective properties of soft acoustic metamaterials including negative index," Sci. Rep. **5**, 18562 (2015).
[26]D. Torrent and J. Sanchez-Dehesa, "Multiple scattering formulation of two-dimensional acoustic and electromagnetic metamaterials," New J. Phys. **13**, 093018 (2011).
[27]M. J. W. Povey, "Ultrasound particle sizing: A review," Particuology **11**, 135–147 (2013).
[28]M. Su, M. Xue, X. Cai, Z. Shang, and F. Xu, "Particle size characterization by ultrasonic attenuation spectra," Particuology **6**, 276–281 (2008).
[29]A. K. Hipp, G. Storti, and M. Morbidelli, "Particle sizing in colloidal dispersions by ultrasound. Model calibration and sensitivity analysis," Langmuir **15**, 2338–2345 (1999).
[30]F. Babick, M. Stintz, and A. Richter, "Ultrasonic particle sizing of disperse systems with partly unknown properties," Part. Part. Syst. Char. **23**, 175–183 (2006).
[31]D. J. McClements and J. N. Coupland, "Theory of droplet size distribution measurements in emulsions using ultrasonic spectroscopy," Colloids Surf. A **117**, 161–170 (1996).
[32]P. Mougin, A. Thomas, D. Wilkinson, G. White, K. J. Roberts, N. Herrmann, R. Jack, and R. Tweedie, "On-line monitoring of a crystallization process," AIChE J. **49**, 373–378 (2003).
[33]A. K. Hipp, B. Walker, M. Mazzotti, and M. Morbidelli, "*In-situ* monitoring of batch crystallization by ultrasound spectroscopy," Ind. Eng. Chem. Res. **39**, 783–789 (2000).
[34]P. Frohberg and J. Ulrich, "Single-frequency ultrasonic crystallization monitoring (UCM): Innovative technique for in-line analyzing of industrial crystallization processes," Org. Proc. Res. Dev. **19**, 84–88 (2015).
[35]M. Xue, M. Su, L. Dong, Z. Shang, and X. Cai, "An investigation on characterizing dense coal-water slurry with ultrasound: Theoretical and experimental method," Chem. Eng. Commun. **197**, 169–179 (2009).
[36]A. S. Dukhin, P. J. Goetz, and T. G. M. v. de Ven, "Ultrasonic characterization of proteins and blood cells," Colloids Surf. B **53**, 121–126 (2006).
[37]A. S. Dukhin and P. J. Goetz, *Ultrasound for Characterizing Colloids: Particle Sizing, Zeta Potential, Rheology* (Elsevier, Amsterdam, 2002).
[38]A. Aubry and A. Derode, "Ultrasonic imaging of highly scattering media from local measurements of the diffusion constant: Separation of coherent and incoherent intensities," Phys. Rev. E **75**, 026602 (2007).
[39]V. Leroy and A. Derode, "Temperature-dependent diffusing acoustic wave spectroscopy with resonant scatterers," Phys. Rev. E **77**, 036602 (2008).
[40]N. Viard and A. Derode, "Measurements of ultrasonic diffusivity and transport speed from coda waves in a resonant multiple scattering medium," J. Acoust. Soc. Am. **138**, 134–145 (2015).
[41]M. L. Cowan, J. H. Page, and P. Sheng, "Ultrasonic wave transport in a system of disordered resonant scatterers: Propagating resonant modes and hybridization gaps," Phys. Rev. B **84**, 094305 (2011).
[42]R. Weser, S. Woeckel, B. Wessely, and U. Hempel, "Particle characterisation in highly concentrated dispersions using ultrasonic backscattering method," Ultrasonics **53**, 706–716 (2013).
[43]R. Weser, S. Woeckel, B. Wessely, U. Steinmann, F. Babick, and M. Stintz, "Ultrasonic backscattering method for *in-situ* characterisation of concentrated dispersions," Powder Technol. **268**, 177–190 (2014).

[44]L. L. Foldy, "The multiple scattering of waves," Phys. Rev. **67**, 107–119 (1945).
[45]P. C. Waterman and R. Truell, "Multiple scattering of waves," J. Math. Phys. **2**, 512–537 (1961).
[46]J. G. Fikioris and P. C. Waterman, "Multiple scattering of waves. II. 'Hole corrections' in the scalar case," J. Math. Phys. **5**, 1413–1420 (1964).
[47]P. Lloyd and M. V. Berry, "Wave propagation through an assembly of spheres. IV. Relations between different multiple scattering theories," Proc. Phys. Soc. London **91**, 678–688 (1967).
[48]R. E. Challis, M. J. W. Povey, M. L. Mather, and A. K. Holmes, "Ultrasound techniques for characterizing colloidal dispersions," Rep. Prog. Phys. **68**, 1541–1637 (2005).
[49]A. K. Hipp, G. Storti, and M. Morbidelli, "Acoustic characterization of concentrated suspensions and emulsions. 2. Experimental validation," Langmuir **18**, 405–412 (2002).
[50]S. Meyer, S. Berrut, T. I. J. Goodenough, V. S. Rajendram, V. J. Pinfield, and M. J. W. Povey, "A comparative study of ultrasound and laser light diffraction techniques for particle size determination in dairy beverages," Meas. Sci. Technol. **17**, 289–297 (2006).
[51]M. J. W. Povey, "Crystal nucleation in food colloids," Food Hydrocoll. **42**, 118–129 (2014).
[52]D. J. McClements, "Critical review of techniques and methodologies for characterization of emulsion stability," Crit. Rev. Food Sci. Nutr. **47**, 611–649 (2007).
[53]R. E. Challis, A. K. Holmes, and V. Pinfield, "Ultrasonic bulk wave propagation in concentrated heterogeneous slurries," in *Ultrasonic Wave Propagation in Non Homogeneous Media*, edited by A. Leger and M. Deschamps (Springer-Verlag, Berlin, 2009), pp. 87–98.
[54]R. E. Challis and V. J. Pinfield, "Ultrasonic wave propagation in concentrated slurries—The modelling problem," Ultrasonics **54**, 1737–1744 (2014).
[55]P. S. Epstein and R. R. Carhart, "The absorption of sound in suspensions and emulsions. I. Water fog in air," J. Acoust. Soc. Am. **25**, 553–565 (1953).
[56]J. R. Allegra and S. A. Hawley, "Attenuation of sound in suspensions and emulsions: Theory and experiments," J. Acoust. Soc. Am. **51**, 1545–1564 (1972).
[57]A. K. Hipp, G. Storti, and M. Morbidelli, "Acoustic characterization of concentrated suspensions and emulsions. 1. Model analysis," Langmuir **18**, 391–404 (2002).
[58]M. A. Isakovich, "Propagation of sound in emulsions," Zh. Eksp. I Teor. Fiz. **18**, 907–912 (1948).
[59]Y. Hemar, N. Herrmann, P. Lemarechal, R. Hocquart, and F. Lequeux, "Effective medium model for ultrasonic attenuation due to the thermo-elastic effect in concentrated emulsions," J. Phys. II **7**, 637–647 (1997).
[60]D. J. McClements, Y. Hemar, and N. Herrmann, "Incorporation of thermal overlap effects into multiple scattering theory," J. Acoust. Soc. Am. **105**, 915–918 (1999).
[61]F. Alba, "Novel fundamental model for the prediction of multiply scattered generic waves in particulates," in *Concentrated Dispersions*, edited by P. Somasundaran and B. Markovic (American Chemical Society, New York, 2004), pp. 135–148.
[62]F. Luppé, J. M. Conoir, and A. N. Norris, "Effective wave numbers for thermo-viscoelastic media containing random configurations of spherical scatterers," J. Acoust. Soc. Am. **131**, 1113–1120 (2012).
[63]V. J. Pinfield, "Thermo-elastic multiple scattering in random dispersions of spherical scatterers," J. Acoust. Soc. Am. **136**, 3008–3017 (2014).
[64]V. J. Pinfield, "Advances in ultrasonic monitoring of oil-in-water emulsions," Food Hydrocoll. **42**, 48–55 (2014).
[65]D. M. Forrester, J. Huang, V. J. Pinfield, and F. Luppé, "Experimental verification of nanofluid shear-wave reconversion in ultrasonic fields," Nanoscale **8**, 5497–5506 (2016).
[66]D. M. Forrester, J. Huang, and V. J. Pinfield, "Characterisation of colloidal dispersions using ultrasound spectroscopy and multiple-scattering theory inclusive of shear-wave effects," Chem. Eng. Res. Design **114**, 69–78 (2016).
[67]N. G. Einspruch, E. J. Witterholt, and R. Truell, "Scattering of a plane transverse wave by a spherical obstacle in an elastic medium," J. Appl. Phys. **31**, 806–818 (1960).
[68]V. J. Pinfield, "Acoustic scattering in dispersions: Improvements in the calculation of single particle scattering coefficients," J. Acoust. Soc. Am. **122**, 205–221 (2007).
[69]R. E. Challis, J. S. Tebbutt, and A. K. Holmes, "Equivalence between three scattering formulations for ultrasonic wave propagation in particulate mixtures," J. Phys. D **31**, 3481–3497 (1998).
[70]M. Caleap, B. W. Drinkwater, and P. D. Wilcox, "Coherent acoustic wave propagation in media with pair-correlated spheres," J. Acoust. Soc. Am. **131**, 2036–2047 (2012).
[71]A. Derode, V. Mamou, and A. Tourin, "Influence of correlations between scatterers on the attenuation of the coherent wave in a random medium," Phys. Rev. E **74**, 036606 (2006).
[72]V. Pinfield and D. Forrester, "Shear-acoustic multiple scattering silica in water data," JASA 2017. figshare. DOI: 10.17028/rd.lboro.3465764.